frontiers | Frontiers in Plant Science

TYPE Original Research
PUBLISHED 14 December 2023
DOI 10.3389/fpls.2023.1327385

OPEN ACCESS

EDITED BY
Giao Nguyen,
Department of Primary Industries and Regional Development of Western Australia (DPIRD), Australia

REVIEWED BY
Filippos Bantis,
University of Patras, Greece
Fan Xxiaoxue,
Jiangsu Academy of Agricultural Sciences (JAAS), China

*CORRESPONDENCE
Rubén Moratiel
ruben.moratiel@upm.es

RECEIVED 24 October 2023
ACCEPTED 30 November 2023
PUBLISHED 14 December 2023

CITATION
Moratiel R, Jimenez R, Mate M, Ibánez MA, Moreno MM and Tarquis AM (2023) Net CO_2 assimilation rate response of tomato seedlings (*Solanum lycopersicum* L.) to the interaction between light intensity, spectrum and ambient CO_2 concentration.
Front. Plant Sci. 14:1327385.
doi: 10.3389/fpls.2023.1327385

Net CO_2 assimilation rate response of tomato seedlings (*Solanum lycopersicum* L.) to the interaction between light intensity, spectrum and ambient CO_2 concentration

Rubén Moratiel[1,2]*, Raúl Jimenez[2,3], Miriam Mate[4], Miguel Angel Ibánez[5], Marta M. Moreno[6] and Ana M. Tarquis[1,7]

[1]CEIGRAM, Universidad Politécnica de Madrid, Madrid, Spain, [2]AgSystems, ETSI Agronómica, Alimentaria y Biosistemas, Universidad Politécnica de Madrid, Madrid, Spain, [3]Entomología Aplicada a la Agricultura y la Salud, Departamento de Biotecnología Microbiana y de Plantas, Centro de Investigaciones Biológicas Margarita Salas (CIB), CSIC, Madrid, Spain, [4]ICEI, Universidad Complutense de Madrid, Pozuelo de Alarcón, Madrid, Spain, [5]Departamento Economía Agraria, Estadística y Gestión de Empresas, Escuela Técnica Superior de Ingeniería Agronómica, Alimentaria y de Biosistemas, Universidad Politécnica de Madrid (UPM), Ciudad Universitaria, Madrid, Spain, [6]University of Castilla-La Mancha, Higher Technical School of Agricultural Engineering in Ciudad Real, Ciudad Real, Spain, [7]Grupo de Sistemas Complejos, Universidad Politécnica de Madrid, Madrid, Spain

Artificial lighting is complementary and single-source lighting for controlled Environment Agriculture (CEA) to increase crop productivity. Installations to control CO_2 levels and luminaires with variable spectrum and intensity are becoming increasingly common. In order to see the net assimilation of CO_2 based on the relationship between the three factors: intensity, spectrum and CO_2 concentration, tests are proposed on tomatoes seedling with combinations of ten spectra (100B, 80B20G, 20B80G, 100G, 80G20R, 20G80R, 100R, 80R20B, 20R80B, 37R36G27B) seven light intensities (30, 90, 200, 350, 500, 700 and 1000 $\mu mol \cdot m^{-2}\ s^{-1}$) and nine CO_2 concentrations (200, 300, 400, 500, 600, 700, 800 and 900 ppm). These tomato seedlings grew under uniform conditions with no treatments applied up to the moment of measurement by a differential gas analyzer. We have developed a model to evaluate and determine under what spectrum and intensity of light photosynthesis the Net assimilation of CO_2 (A_n) is more significant in the leaves of tomato plants, considering the CO_2 concentration as an independent variable in the model. The evaluation of the model parameters for each spectrum and intensity shows that the intensity has a more decisive influence on the maximum A_n rate than the spectra. For intensities lower than 350 $\mu mol \cdot m^{-2}\ s^{-1}$, it is observed that the spectrum has a greater influence on the variable A_n. The spectra with the best behaviour were 80R20B and 80B20R, which maintained A_n values between 2 and 4 ($\mu mol\ CO_2 \cdot m^{-2} \cdot s^{-1}$) above the spectra with the worst behaviour (100G, 80G20R, 20G80R and 37B36G27R) in practically all situations. Photosynthetic Light-Use Efficiency (PLUE) was also higher for the 80B20R and 20R80B spectra with values of 36,07 and 33,84 mmol $CO_2 \cdot mol\ photon^{-1}$,

respectively, for light intensities of 200 µmol·m^{-2} s^{-1} and 400 ppm of CO_2that increased to values of 49,65 and 48,38 mmol CO_2·mol photon^{-1} for the same light intensity and concentrations of 850 ppm. The choice of spectrum is essential, as indicated by the data from this study, to optimize the photosynthesis of the plant species grown in the plant factory where light intensities are adjusted for greater profitability.

KEYWORDS

photosynthesis, light intensity, light spectrum, CO_2 concentration, net CO_2 assimilation rate, tomato seedling

1 Introduction

Light is one of the major factors that drive photosynthesis and plant development. Light spectra, intensity and duration (light dimensions) are involved in almost all vegetative processes. Among others, photomorphogenesis, phototropism, maintenance of the circadian clock or the Shade-Avoidance Syndrome (SAS) (Trojak et al., 2022). These light dimensions are also directly responsible for the efficiency of photosynthesis and determine the Net CO_2 Assimilation Rate (A_n). This balance fixes plants' photo-assimilate amount and phytochemical content (Spalholz et al., 2020). Since the beginning of the century, scientific publications regarding Light Emitting Diode (LED) illumination in plants have grown exponentially, given the fine-tuning of light that new technology provides (Sipos et al., 2020). This increase manifests the amount of research performed lately, testing the effect of different dimensions of light over many crops (Viršilė et al., 2017; Sipos et al., 2020), which has been proven to be not only species- but even cultivar-dependant, each reacting differently (even though with some general similarities) to the spectra, intensity and photoperiod they were exposed (Bantis et al., 2018; Liang et al., 2021).

Artificial illumination has become relevant in the last decades as supplemental and sole-source illumination for Controlled Environment Agriculture (CEA) to increase crop productivity (Bantis et al., 2018). The recent LED technology development allows not only the reduction of costs and, therefore, the increase of the efficiency of vegetable production but also the establishment of the effect of narrow wavelength spectra over different plant processes, as mentioned above. Moreover, with LED technology, it is possible to change the most important aspects of light that affect plants: photosynthetic photon flux density (PPFD) in the photosynthetically active radiation (PAR) spectral, photoperiod, lighting mode (impulses or continuous) and light spectral composition (Berkovich et al., 2017).

In general, Red (R; 600-700 nm) and Blue (B; 400-500 nm) wavebands (RB) are the most efficient in terms of photosynthesis. They comprehended the *in vitro* absorption peaks of Chlorophyll *a* (430 nm and 662 nm) and Chlorophyll *b* (453 nm and 642 nm) when they were extracted in diethyl ether (Du et al., 1998; Pennisi et al., 2019). That is why different RB light combinations were first used as LED growing illumination (Spalholz et al., 2020; Zheng et al., 2021). Green (G; 500-600 nm) and some wavebands outside the Photosynthetically Active Radiation (PAR; 400-700 nm) range, such as Far Red (FR; 700-800 nm), have only recently started to be taken into consideration for these artificial illumination solutions since they appear to be poorly absorbed by photosynthetic pigments (Zhen et al., 2021). These authors consider that a new definition should replace the definition of PAR (400-700 nm) extended PAR (ePAR,400-750nm), which is more influential in photosynthesis and plant growth and development (Zhen et al., 2021). However, these wavebands are of importance in photosynthesis at conditions of high PPFD due to their higher transmittance within the leaves and canopy or by balancing excitation of Photosystem II (PSII) and Photosystem I (PSI) in the so-called Emmerson effect (Zhen et al., 2019). The effect of these wavelengths over plant development has shifted the light composition of artificial illumination solutions, which are starting to include broad-spectrum LEDs to cover all PAR wavebands and somehow mimic sunlight (Berkovich et al., 2017).

Being able to control the intensity and spectrum that plants receive is crucial in order to harness photosynthetic processes. It is now known that light quantity and quality have an interactive effect on photosynthesis driven by the transmittance and absorption properties of different wavelengths within the PAR spectrum (Terashima et al., 2009). Given the high absorptance of RB by the chlorophylls *in vitro*, it has been commonly accepted that they are the main drivers of photosynthesis, especially when compared to G light (van Iersel, 2017). However, this only seems true under low PPFD conditions when the photosynthetic machinery is not saturated. The low transmittance of RB light does not allow those photons to penetrate deeper leaf layers. So they are absorbed by chlorophylls even when they are already saturated, forcing them to

Abbreviations: A_n, Net CO_2 Assimilation rate; B, Blue photons (400 – 500 nm); G, Green photons (500-600 nm); LED, light-emitting diode; PLUE, Photosynthetic Light-Use Efficiency; PPFD, photosynthetic photon flux density; PAR, photosynthetically active radiation; R, Red photons (600-700 nm).

dissipate that energy non-photochemically on the adaxial layers of the leaf. On the other hand, chlorophylls' low absorptance of G light allows it to reach chloroplast through the whole leaf. Thus increasing the photosynthetic light use efficiency once PPFD is high enough to start saturating the upper layers of leaves (Terashima et al., 2009).

In order to dissect the interactive effect of light quality and intensity, a comprehensive study was presented quantifying the photosynthetic response of lettuce to different combinations of B, G and/or R light over a wide range of intensities (Liu and van Iersel, 2021). It was demonstrated that G photons could drive photosynthesis as efficiently as B light under low PPFD conditions. However, given their low absorptance, G light is generally less efficient in these conditions. However, at high PPFD, the photosynthetic efficiency of G light was similar to R light, not only once absorbed but on a light incident basis, with B light scoring the lowest. Similar behaviour in sunflowers on the effect of the green spectrum was reported by Terashima et al. (2009). Chlorophylls, flavonoids, and carotenoids absorb blue light, which may lead to a lesser photosynthetic yield once chlorophylls are saturated (Sun et al., 1998). This phenomenon occurs to G light on a lower basis, which might explain why R light continues to have the best behaviour. As PPFD increases, the yield for CO_2 assimilation per photon decreases as more energy is dissipated in non-photochemical processes. However, this reduction seems slower under G light than under B or R light, assumably because of the lower absorption of green photons, thus, their better distribution throughout the leaf. This more uniform distribution reduces non-photochemical quenching (NPQ). At the same time, lower penetration of blue and red light upregulates NPQ on the upper parts of the leaves and cannot drive photosynthesis on the lower levels (Liu and van Iersel, 2021). This is important under high PPFD since NPQ is proportional to light intensity (Zhen and van Iersel, 2017).

Tomato (*Solanum lycopersicum* L.) is one of the crops most cultivated worldwide (FAOSTAT, 2022) due to its nutritional characteristics and culinary importance (Dorais et al., 2008). It is also a model plant for the study of the effect of light on plants in controlled environments, given its responsiveness to light (Yang et al., 2018). Light availability in greenhouse crops along seasons is a growing concern in northern latitudes and meridional areas such as the Mediterranean. It has been proven that supplemental LED inter-lighting illumination (R:B, 3:1) results in larger and heavier tomato fruits, especially in seasons with lower solar radiation, as well as faster fruit growth and maturation, which in turn results in higher yields (Paucek et al., 2020). This might be due to the photosynthetic capacity and light sensibility of unripped tomato fruits, which have been shown to increase their melatonin levels under RB light, a novel plant hormone that seems to promote ripening by inducing ethylene production and protect against senescence by scavenging reactive oxygen species (Li et al., 2021)

The main climate factors determining plant growth are ePAR light (Zhen et al., 2021), air temperature, air humidity, CO_2 concentration, wind, root temperature, nutrient availability, water and oxygen. The chemical reaction of photosynthesis can be simplified as follows (Equation 1):

$$light\ \ energy + \ 6CO_2 + 12H_2O = C_6H_{12}O_6 + 6O_2 + 6H_2O \quad (1)$$

Carbon dioxide is one of the substrates for photosynthesis. Thus, it can be a limiting factor for the reaction when its concentration is below optimal. According to the Law of Minimum (also known as Liebig Law), varying only the light energy plants receive may not be enough to enhance photosynthesis properly since it is not the only substrate of the reaction. Thus, it is necessary to consider ambient CO_2 to evaluate the photosynthetic efficiency of a given light source, adding a new dimension to the light quality and intensity interactive effect. In protected crop conditions, the environmental factors modified last are CO_2 and lighting, the temperature and relative humidity being the first to be controlled.

In this study, we aim to identify how light intensity, its spectrum and concentration of ambient conditions of CO_2 affect the Net CO_2 Assimilation in tomato (*Solanum lycopersicum* L.) plants. Tomato seedlings grew under uniform conditions with no treatments applied up to the moment of measurement. Tomato leaves were exposed to spectra of different combinations of blue, green and/or red light in a wide range of intensities and increasing CO_2 availability to assess the Net CO_2 Assimilation under each ambient condition.

2 Materials and methods

2.1 Plant material

The trials were conducted at the Experimental Field at Agricultural Engineering School of Universidad Politécnica de Madrid (Latitude: 40.439413N; Longitude: 3.737547W) during May-Dic 2021. Tomato (*Solanum lycopersicum* L. cv. *Anairis*) seeds were sown in trays of 36 pots (3 cm length x 3 cm wide x 7 cm depth) filled with seedbed substrate with a mixture composed of 70% of white peat and 30% black peat (Tray 70/30 Gramoflor GmbH & Co. KG, Vechta, Germany) and covered with vermiculite. All plants were cultivated in a glass Greenhouse at the Experimental Field with an ACOM 2019® (Acom, Balsicas, Murcia, Spain) environmental controller. The mean night/day temperature fluctuated between 18-14°C/28-20°C with adifference in day and night temperature (DIF) between +6 and +10°C and humidity between 80-60%. The maximum light intensity in the greenhouses was 400 $\mu molm^{-2}s^{-1}$ (shade screens and application of calcium hydroxide, whitening, on the cover material were used) and day-night photoperiod of 14-10 h. Pots were watered daily as needed, and once a week, a general nutritive solution (5.69 mM $CaNO_3$; 2.77 mM KNO_3; 4.08 mM $MgSO_4$; 1.56 mM K_2PO_4 and 0.048 gL^{-1} Nutrel C micronutrients Yara Inc.), was used to avoid nutrient deprivation. The conductivity of the nutrition solution was 2.1 $dS{\cdot}m^{-1}$ and a pH of 6.2. Seedlings were grown to BBCH (Biologische Bundesanstalt, Bundessortenamt und Chemische Industrie) 14-15, 4-5th leaf on the main shoot unfolded (Feller et al., 1995). One day before taking the measurements, the seedlings were moved to a climatic chamber with a capacity of 350 L (Mod. Hot-Cold GL, JP Selecta, Barcelona, Spain). The conditions in the

10.3389/fpls.2023.1327385

chamber were 25 °C, 80% relative humidity, and PPFD of 400 µmol/m^2·s with the photoperiod 14-10 h day-night.

2.2 Carbon assimilation measurements

Tomato plants were taken for measurements 25-35 days after sowing. Only plants whose at least a fourth true leaf was completely unfolded and whose third true leaf did not show any sign of stress or deprivation were selected for analysis and discarded afterwards. Selected plants were dark-adapted for 30 minutes, and their third leaf was clipped to the leaf cuvette (PLC 3 Universal Leaf cuvette) with a window measuring 25 mm x 7 mm of a gas exchange system (CIRAS-3, PP Systems, Amesbury, MA, USA) provided with a LED Light Unit (RGBW). This dimmable light unit peaks at 446 nm (blue), 523 nm (green) and 653 nm (red) with full width at half maximum (FWHM) of 16, 36 and 17 nm, respectively (Liu and van Iersel, 2021). The combination of blue, green and red light allowed for the composition of 10 different light spectra (Table 1). The three monochromatic spectra of PAR radiation (100B, 100G, 100R), six combinations of binary spectra based on percentages of blue 20%, that are used in supplemental lighting (Kaiser et al., 2019) maintaining the proportions of 20%/80% of all combinations of blue, green and red spectrum and simulated natural light (reference of our study). Three plants were measured per spectrum. Each light spectrum was tested at seven different light intensities (30, 90, 200, 350, 500, 700 and 1000 µmol·m^{-2} s^{-1}).

Different spectra were designed so it would be possible to determine the effect of each monochromatic light as well as their interaction by pairs. A trichromatic spectrum was designed to average the light a plant would receive on a sunny summer day. Therefore, solar radiation was recorded in triplicate at three different moments of a sunny summer day (morning, noon and evening) using a spectroradiometer (PN-200, UPRtek, Zhunan Township, Miaoli County, Taiwan) and those nine readings were averaged. The resulting spectrum was then divided into segments of 100 nm, and the fraction Blue (400-499 nm), Green (500-599 nm) and Red (600-699 nm) was calculated and used to design the trichromatic spectrum (Figure 1).

TABLE 1 Light composition of each spectrum used in the study.

Spectra	Fraction of photon flux (%)		
	Blue	Green	Red
100B	100	0	0
80B20G	80	20	0
20B80G	20	80	0
100G	0	100	0
80G20R	0	80	20
20G80R	0	20	80
100R	0	0	100
80R20B	20	0	80
20R80B	80	0	20
37R36G27B	37	36	27

To study the photosynthesis efficiency under different spectra, intensities, and CO_2 concentrations, we constructed CO_2 response curves for each intensity and spectrum using a Rapid A/Ci Response (RACiR) technique (Saathoff and Welles, 2021). The photosynthetic light-use efficiency (PLUE) was calculated, which is defined as the slope between the net CO_2 assimilation rate (A_n) and incident PPFD on the leaf.

After 5 minutes of acclimatization in the lowest CO_2 concentration and light intensity (200 ppm CO_2, 30 µmol·m^{-2}·s^{-1} photons), three Net CO_2 Assimilation rates (A_n), Stomatic Conductance, Vapour Pressure Deficit (VPD) and Water Use Efficiency (WUE) readings were taken at a 10 seconds interval. CO_2 concentration was then raised to 100 ppm, and the leaf was kept in these conditions for two minutes before recording the three readings. This continued through all the CO_2 concentrations studied (200, 300, 400, 500, 600, 700, 800 and 900 ppm). Once the maximum concentration is reached, the light intensity rises to the next lowest intensity of the study. CO_2 concentration then decreases by 100 ppm per triplicate of readings until the lowest concentration is reached, and then light intensity rises again. This process is repeated until all light intensities (30, 90, 200,350, 500, 700 and 1000 µmol·m^{-2}·s^{-1}) are reached. Recordings are taken for every CO_2 concentration and light intensity in the study (Table 2). Environmental conditions inside the cuvette were controlled by the leaf gas exchange system setting values of leaf temperature of 25.0 ± 0.4°C and VPD of 1.6 ± 0.3kPa.

2.3 Statistical analysis

A nonlinear mixed effects model (Lindstrom and Bates, 1990) was estimated to relate assimilation rate as a response variable and light spectra, light intensity and CO_2 concentration levels as explanatory variables.

An asymptotic regression model was used to describe limited growth, where the response variable approaches a horizontal asymptote as CO_2 approaches infinity.

The model used was:

$$A_n = c + (d - c) \times (1 - e^{-\frac{CO_2}{b}}) \quad (2)$$

Where

A_n is the Net CO_2 Assimilation rate, c is the value of A_n when the CO_2 level is zero, d is the maximum attainable A_n, 1/b is proportional to A_n's relative rate of increase as CO_2 increases, and e is a random error term. This term (e) was assumed to have a normal distribution with zero mean and different variance for each intensity level.

It is assumed that the values of c, d and e depend on the light spectra and intensity levels.

c = Intensity + Spectra

d = Intensity + Spectra + u

b = Intensity + Spectra

10.3389/fpls.2023.1327385

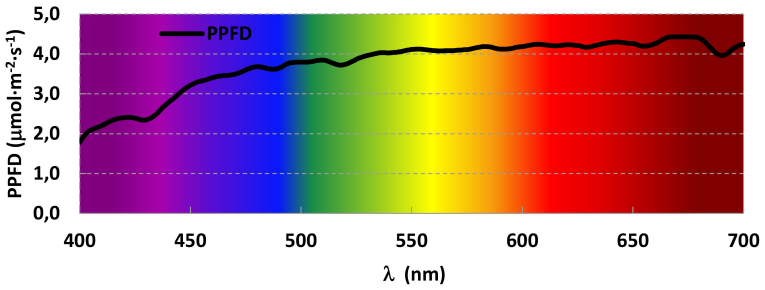

FIGURE 1
Averaged solar radiation in the interval of photosynthetic active radiation (PAR) during a sunny summer day (August 6, 2021) in the Experimental Field in Madrid, Spain (Latitude: 40.439413 N, Longitude: 3.737547W).

where u is a random term that considers the variability for each plant in the parameter d. The random term u was assumed to have a normal distribution with mean 0 and variance σ_u^2.

The statistical model, as defined, took into account the hierarchical structure in which the data was obtained: Three plants per spectrum were measured, and each plant was tested at different light intensities and CO_2 concentrations. The experimental data estimated the parameters b, c and d based on the intensity and spectrum levels used. Hypothesis tests were performed to determine significant differences between their estimates and standard errors. Normality assumptions were also checked using the residuals of the estimated model. The bigger the b parameter, the lower the curvature; hence, the higher the theoretical CO_2 saturation point. The more intensity applied, the higher the d parameter and the highest theoretical maximum A_n is reached. This model studies the effect of the different spectra and intensities over the c, d and b parameters.

Statistical analysis was performed in the R environment (R Core Team, 2021). The model estimation was done with the *nlme* package (Pinheiro et al., 2021), a testing hypothesis was carried out with the *emmeans* package (Russell, 2022) and graphics with the ggplot package (Wickham, 2009).

TABLE 2 Environmental conditions (CO_2 Concentration and Light Intensity) were set for each set of three readings (N) during measurements.

N	[CO_2] (ppm)	I (µmol·m^{-2}·s^{-1})	N	[CO_2] (ppm)	I (µmol·m^{-2}·s^{-1})	N	[CO_2] (ppm)	I (µmol·m^{-2}·s^{-1})
1	200	30	20	500	200	39	800	500
2	300	30	21	600	200	40	900	500
3	400	30	22	700	200	41	900	700
4	500	30	23	800	200	42	800	700
5	600	30	24	900	200	43	700	700
6	700	30	25	900	350	44	600	700
7	800	30	26	800	350	45	500	700
8	900	30	27	700	350	46	400	700
9	900	90	28	600	350	47	300	700
10	800	90	29	500	350	48	200	700
11	700	90	30	400	350	49	200	1000
12	600	90	31	300	350	50	300	1000
13	500	90	32	200	350	51	400	1000
14	400	90	33	200	500	52	500	1000
15	300	90	34	300	500	53	600	1000
16	200	90	35	400	500	54	700	1000
17	200	200	36	500	500	55	800	1000
18	300	200	37	600	500	56	900	1000
19	400	200	38	700	500			

This has been performed over three plants per spectrum described in Table 1.

3 Results

3.1 Changes in net carbon assimilation due to varying CO_2 concentration, light intensity and spectra used

Net Carbon Assimilation (A_n) was assessed at eight different CO_2 concentrations for seven light intensity values at ten light spectra varying R, G and B light fractions (Figure 2) on the third true leaf of tomato plants. For every spectrum, at light intensities of 200 $\mu mol \cdot m^{-2} \cdot s^{-1}$ or higher, A_n/CO_2-concentration response showed the typical display of an asymptotic curve, A_n rising rapidly as CO_2 increased at lower levels until reaching a concentration in which A_n increase slows down and even stops going up. The higher the intensity, the higher the curvature, reaching higher A_n values in all spectra. At lower light intensities (30 and 90 $\mu mol \cdot m^{-2} \cdot s^{-1}$), CO_2 response curves were more lineal, not showing a pronounced change in the tendency of the curve. The curves' shapes were similar at all the spectra and intensities used, pointing out the same A_n behaviour due to increases in CO_2 concentration. However, the absolute values of A_n changed through different spectra. The highest A_n values at every light intensity were observed at 20R80B and 80R20B spectrums. The lowest A_n values were archived by the 20G80R spectrum, followed by the trichromatic spectrum 37R36G27B (Figure 2). The highest A_n values, 18.9 $\mu mol\ CO_2 \cdot m^{-2} \cdot s^{1}$, were obtained at CO_2 concentrations of 700, 800 and 900 ppm, and with 1000 $\mu mol \cdot m^{-2} \cdot s^{-1}$ light intensity and in 80R20B spectrum. Contrary, the A_n lowest values, -4.9 and -3.2 $\mu mol\ CO_2 \cdot m^{-2} \cdot s^{-1}$, were reached in 100 G and 20G80R spectrums, and CO_2 intensities of 30 $\mu mol \cdot m^{-2} \cdot s^{-1}$ and 200 ppm, respectively.

3.2 Model

The most frequently used methods to understand how C_3 plant photosynthesis responds to changes in CO_2 concentration are based on the studies of Farquhar et al. (1980). These biochemical models focus on the activity of ribulose 1:5 bisphosphate carboxylase/oxygenase (Rubisco). We have developed a model to determine under which light photosynthesis spectrum and intensity is greater for tomato plants' leaves, considering the concentration of CO_2 as an independent variable.

Table 3 studies the interference of the model with the intensity of illumination. The simulated solar spectrum of 37R36G27B is a reference for the analysis. The intensity of 350 $\mu mol \cdot m^{-2} \cdot s^{-1}$ is used as a reference to analyze the spectra (Table 4). The same trend is observed in each spectrum or intensity compared. It shows an increase or decrease of the parameters by the same amount (Table 5).

In the analyses carried out in the model, one of the most important parameters is to determine *d* (asymptotic value of maximum A_n when the CO_2 concentration tends to infinity), with a higher value of *d*, higher production potential. Table 3 shows the estimated values of *d* for each lighting intensity level. It is observed that there is a positive relationship between the intensity and the values of d. The increase in intensity tends to increase the estimated value of the parameter *d*. The highest intensities, 700 and 1000 $\mu mol \cdot m^{-2} \cdot s^{-1}$, show the highest values of parameter d (12.01 and 11.98, respectively), showing significant differences for the other intensities. This trend would be observed regardless of the spectrum used, decreasing or increasing the estimated values by the same amount depending on the spectrum used. The estimated values

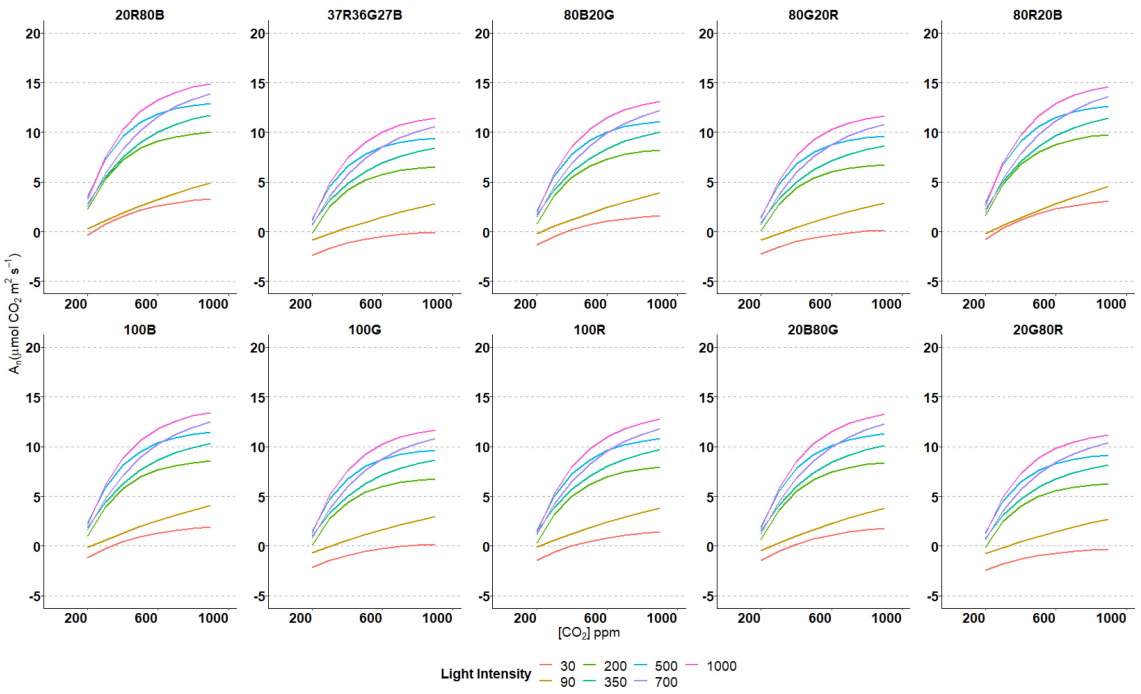

FIGURE 2
Estimated nonlinear regression models for A_n and CO_2 concentrations at different intensities and spectrums used.

TABLE 3 Mean parameters *d* and *b* values from the model (Equation 2) for every intensity examined in the spectrum 37R36G27B.

Intensity (µmol·m^{-2}·s^{-1})	*d* (± s.e.)		*b* (± s.e.)	
30	0.26^{a}	± 0.42	320.71^{abc}	± 43.90
200	6.74^{bcd}	± 0.39	202.98^{abc}	± 8.13
90	7.73^{bcd}	± 1.50	1264.96^{d}	± 249.9
350	9.28^{c}	± 0.42	310.32^{c}	± 16.08
500	9.68^{c}	± 0.39	202.34^{a}	± 7.83
1000	11.98^{d}	± 0.4	231.78^{b}	± 8.61
700	12.01^{d}	± 0.4	333.32^{c}	± 17.34

Mean values ± standard error. Mean values that include a common letter in the same column are not statistically different (p ≤ 0.05).

of parameter *b* (responsible for curvature) fluctuate between 202.34 for 500 µmol·m^{-2}·s^{-1} and 1264.96 for 90 µmol·m^{-2}·s^{-1} (Table 3). Note that all the intensities, except for 90 µmol·m^{-2}·s^{-1}, are between 200 and 340. For intensity of 90 µmol·m^{-2}·s^{-1}, very high *b* values are observed, indicating that it practically approaches its maximum linearly. At higher values of *b*, the curve tends to be more linear and needs higher levels of CO_2 to reach its maximum asymptotic value. It is observed that the *b* values do not follow an intensity pattern. However, at low intensities (30 and 90 µmol·m^{-2}·s^{-1}), this parameter shows more significant fluctuations, as the standard error values point out, being much higher than those of the higher intensities (Table 3).

Table 4 shows the model's behaviour depending on the light spectrum for an intensity of 350 µmol·m^{-2}·s^{-1}. As a function of the spectrum, the d and b parameters range values are 8.96 to 12.82 and 305.77 to 334.68, respectively. These values are significantly lower than those required by the light intensity (*d* from 0.26 to 12.01 and *b* from 202.34 to 1264.96). It is observed how the spectra 80R20B and 20R80B are the ones that would reach the highest potential values of A_n, with significant differences concerning the other spectra. The spectrum that reaches the lowest maximum A_n are 20G80R, 37R36G27B, 80G20R, 100G and 100R, with no significant differences (Table 4). Parameter *b* is a parameter with few fluctuations due to the spectra, with no significant differences between 20G80R, 37R36G27B, 80G20R, 100G 80B20G, 20B80G, 100B, 80R20B and 20R80B. In addition, another group is formed by 80B20G, 20B80G, 100B, 80R20B, 20R80B and 100R without significant differences.

Table 5 shows the model parameter values (*d*, *b and c)* for each light intensity and spectrum used in this experiment. Trichromatic spectrum 37R36G27B at 350 µmol·m^{-2}·s^{-1} has been chosen as a reference since it was designed as sunlight radiation. Its values have been used as the baseline. The curve can be obtained for each intensity and spectrum in Table 5.

Figure 3 compares the models with two PPFDs and two spectra. It is observed how the -PPFD component influences more than the spectra. However, the spectra show different trends with the same intensity, observing differences in A_n among them.

When applying values from Table 5 to Equation 2. values for A_n can be calculated for each intensity and spectrum for any fixed CO_2 concentration (Table 6). This work is particularised for three possible scenarios of CO_2 concentration taken into consideration based on different real-life scenarios that can occur under a greenhouse (Both et al., 2017). The first scenario is the study of the A_n of the spectra for the atmospheric concentration (400 ppm), and the second case is the increase in carbon fertilization up to

TABLE 4 Mean ± values of parameters *d* and *b* from the model (Equation 2) for every spectrum light intensity of 350 µmol·m^{-2}·s^{-1}.

Spectra	*d* (± s.e.)		*b* (± s.e.)	
80R20G	8.96^{a}	± 0.42	305.77^{a}	± 16.07
37R36G27B	9.28^{a}	± 0.42	310.32^{a}	± 16.08
20R80G	9.49^{ab}	± 0.42	308.37^{a}	± 16.04
100G	9.51^{ab}	± 0.42	310.90^{a}	± 16.03
100R	10.85^{ab}	± 0.42	334.68^{b}	± 16.21
20G80B	11.06^{cd}	± 0.42	321.73^{ab}	± 16.06
80G20B	11.27^{cd}	± 0.42	325.59^{ab}	± 16.02
100B	11.41^{cd}	± 0.42	320.69^{ab}	± 16.02
80R20B	12.63^{de}	± 0.43	321.12^{ab}	± 15.91
20R80B	12.82^{e}	± 0.42	314.45^{ab}	± 15.88

Mean values ± standard error (s.e.). Mean values that include a common letter in the same column are not statistically different (p ≤ 0.05).

10.3389/fpls.2023.1327385

TABLE 5 Values of parameters *d*, *b* and *c* from the model of Equation 2 for every spectrum and intensity tested.

Spectra	Parameter	Intensities (µmol·m^{-2}·s^{-1})							
		30	90	200	350	500	700	1000	Δ
37R36G27B	***d***	0.26	7.73	6.74	9.28	9.68	12.01	11.98	-
	b	320.71	1264.96	202.98	310.32	202.34	333.32	231.78	-
	c	-4.62	-2.34	-11.61	-6.89	-12.88	-8.76	-13.74	-
100B	***d***	2.39	9.86	8.87	11.41	11.81	14.14	14.11	2.13
	b	331.08	1275.33	213.35	320.69	212.71	343.69	242.15	10.37
	c	-4.12	-1.84	-11.11	-6.39	-12.39	-8.26	-13.24	0.50
100G	***d***	0.49	7.96	6.97	9.51	9.91	12.24	12.21	0.23
	b	321.3	1265.55	203.57	310.91	202.93	333.91	232.37	0.59
	c	-4.45	-2.17	-11.45	-6.73	-12.72	-8.60	-13.57	0.17
100R	***d***	1.83	9.3	8.31	10.85	11.25	13.58	13.55	1.57
	b	345.07	1289.32	227.34	334.68	226.7	357.68	256.14	24.36
	c	-3.97	-1.69	-10.96	-6.24	-12.23	-8.11	-13.09	0.65
20B80G	***d***	2.25	9.72	8.73	11.27	11.67	14.00	13.97	1.99
	b	335.98	1280.23	218.25	325.59	217.61	348.59	247.05	15.27
	c	-4.50	-2.22	-11.49	-6.77	-12.76	-8.64	-13.62	0.12
20G80R	***d***	-0.06	7.41	6.42	8.96	9.36	11.69	11.66	-0.32
	b	316.17	1260.42	198.44	305.78	197.8	328.78	227.24	-4.54
	c	-4.47	-2.19	-11.46	-6.74	-12.73	-8.61	-13.59	0.15
20R80B	***d***	3.8	11.27	10.28	12.82	13.22	15.55	15.52	3.54
	b	324.85	1269.1	207.12	314.46	206.48	337.46	235.92	4.14
	c	-3.88	-1.60	-10.87	-6.15	-12.14	-8.02	-13.00	0.74
80B20G	***d***	2.04	9.51	8.52	11.06	11.46	13.79	13.76	1.78
	b	332.13	1276.38	214.4	321.74	213.76	344.74	243.2	11.42
	c	-4.11	-3.60	-3.09	-2.58	-2.07	-1.56	-1.05	0.51
80G20R	***d***	0.47	7.94	6.95	9.49	9.89	12.22	12.19	0.21
	b	318.76	1263.01	201.03	308.37	200.39	331.37	229.83	-1.95
		-4.63	-4.64	-4.65	-4.66	-4.67	-4.68	-4.69	-0.01
80R20B	***d***	3.6	11.07	10.08	12.62	13.02	15.35	15.32	3.34
	b	331.52	1275.77	213.79	321.13	213.15	344.13	242.59	10.81
	c	-4.44	-2.16	-11.43	-6.71	-12.70	-8.58	-13.56	0.18

Δ show the change rate of that parameter with baseline 37R36G27B spectrum and 350 µmol·m^{-2}·s^{-1}.

levels of 850 ppm, a situation that can be frequently reached in the carbon fertilization of greenhouses of crops of C_3 metabolism like rose and tomato. The last scenario is the reduction of the CO_2 concentration to levels of 200 ppm, a situation that can occur at certain times of the day with poor ventilation in greenhouses and a high rate of photosynthesis in crops with high LAI (Leaf Area Index).

Blue-containing spectra show higher A_n values than their Red and Green counterparts, followed by red-containing spectra. G light seems to have a lower effect in enhancing Net Carbon Assimilation. The highest values for A_n are archived by the 20R80B spectrum, followed by the 80R20B spectrum and then by the monochromatic 100B compared to other spectra at the same light intensity and CO_2 concentrations. The lowest A_n values belong to the 20G80R spectrum, followed by the trichromatic 37R36G27B. Table 6 shows that under conditions of low CO_2 concentration (200 ppm), the A_n values begin to be positive at incident PPFD of 200 µmol·m^{-2}·s^{-1}, although spectra such as 20R80B take positive

10.3389/fpls.2023.1327385

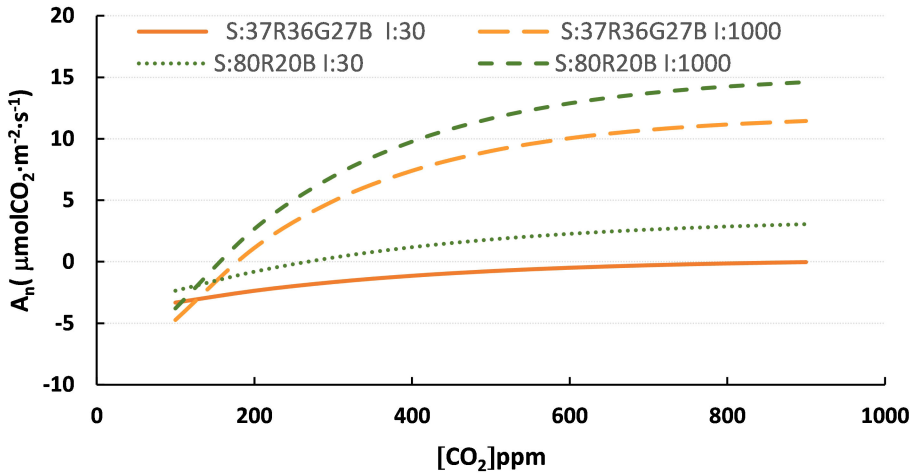

FIGURE 3
Curves of the spectra model 80R20B and R37G36B27 and PPFD of 30 and 1000 µmol·m^{-2}·s^{-1}. S:R37G36B27 I:30, spectra R37G36B27 at 30 µmol·m^{-2}·s^{-1}; S:R37G36B27 I:1000, spectra R37G36B27 at 1000 µmol·m^{-2}·s^{-1}; S: 80R20B I:30, spectra 80R20B at 30 µmol·m^{-2}·s^{-1} and S:80R20B I:1000, spectra 80R20B at 1000 µmol·m^{-2}·s^{-1}.

values at 90 µmol·m^{-2}·s^{-1}. The A_n values do not exceed 4 µmolCO_2·m^{-2}·s^{-1} at these CO_2 concentrations and any PPFD. The highest values are reached in the 80R20B and the 20R80B spectra (2.66 and 3.31, respectively).

For values of 400 ppm of CO_2, even at intensities of 30 µmol·m^{-2}·s^{-1}, positive A_n values are observed for all spectra except for 37R36G27B, 100G and 20G80R. For concentrations of 400 ppm of CO_2 with PPFD of 350 µmol·m^{-2}·s^{-1}, the spectra that reached 7 µmol CO_2·m^{-2}·s^{-1} were 80R20B and 20R80B. The same trend is obtained for these two spectra at concentrations of 850 ppm of CO_2 and 350 µmol·m^{-2}·s^{-1} of PPFD, where they are the only ones that reach 11 µmolCO_2·m^{-2}·s^{-1} of A_n.

In Table 7, a relative comparison is made taking as reference the A_n of 350 µmol·m^{-2}·s^{-1}, with 400 ppm of CO_2 and spectrum of 37R36G27B (with a value of 4.82 µmolCO_2·m^{-2}·s^{-1}) and determined the percentages related to this situation Equation 3. The values shown result from the value obtained as a reference minus the value divided by the reference and multiplied by 100. In this case, it can be seen how the values of the 20R80B and 80R20B spectra are always higher than the reference and other spectra, although it will depend on the PPFD and the CO_2 concentration. The 20R80B and 80R20B spectra with a lower light intensity of 150 µmol·m^{-2}·s^{-1} than the reference (reference with 350 µmol·m^{-2}·s^{-1} and type of spectra with 200 µmol·m^{-2}·s^{-1}) show values of A_n that are 50 and 40% higher, respectively.

$$A_{n\ relative} = 100 * \left(\frac{A_{n\ i} - A_{n\ reference}}{A_{n\ reference}} \right) \qquad [3]$$

Where

$A_{n\ reference}$ = Value of A_n with spectrum 37R36G27B with a PPFD of 350 µmol·m^{-2}·s^{-1} and CO_2 concentration of 400 ppm. A_{ni} = Value of A_n with spectra, PPFD and CO_2 concentrations selected according to Table 6.

Although the relative increases in A_n are marked mainly by the intensity of light and the concentration of CO_2. Table 7 shows the spectra's influence on the Net Carbon Assimilation. Values in A_n with PPFD conditions of 1000 µmol·m^{-2}·s^{-1} and 400 ppm of CO_2 in the 37R36G27B spectrum are similar to those obtained by the 20R80B and 80R20B spectra at PPFD of 350 µmol·m^{-2}·s^{-1} with 400 ppm of CO_2.

Table 8 shows how the variable PLUE changes depending on the spectrum, intensity, and concentration of CO_2. It is observed that PLUE increases as the concentration of CO_2 increases analyzed. At low concentrations of CO_2 (200 ppm), the highest values of PLUE occur at intensities of 350 µmol·m^{-2}·s^{-1}, while as the concentration of CO_2 increases, the highest efficiency is reached at values of 90 -200 µmol·m^{-2}·s^{-1}. Concerning the spectra, although all of them follow the same behaviour, there are differences between them. The ones that show the best efficiency are the spectrum of 20R80B and 20B80R. Concerning light intensity, maximum PLUE values are shown for all spectra and with 200 ppm CO_2 in values around 200-350 PPFD, as we increase CO_2 to 400 and 850 ppm, the maximum PLUE values drop to 200 and 200-90 PPFD, respectively Table 6. Calculated values (according to Table 5 and Equation 2) of A_n (µmol CO_2·m^{-2}·s^{-1}) for each light intensity and spectrum tested at three CO_2 concentration scenarios: 400 ppm as atmospheric CO_2 concentration, 850 ppm as carbon- fertilized greenhouse concentration, and 200 ppm as the case of a CO_2-deprived ambient due to a high photosynthetic rate.

4 Discussion

Since McCree's work (McCree, 1971), Red and Blue light have been considered the most efficient wavebands for photosynthesis. This correlates with chlorophyll absorption spectra, which peak at about 430 and 660 nm (Viršilė et al., 2017). In the literature, no references have been found that deal jointly with the combination of the three factors of light intensity, spectrum and CO_2 concentrations of the photosynthetic responses of seedlings grown

10.3389/fpls.2023.1327385

TABLE 6 Calculated values (according to Table 5 and Equation 2) of A_n (μmol CO_2·m^{-2}·s^{-1}) for each light intensity and spectrum tested at three CO_2 concentration scenarios: 400 ppm as atmospheric CO_2 concentration, 850 ppm as carbon- fertilized greenhouse concentration, and 200 ppm as the case of a CO_2-deprived ambient due to a high photosynthetic rate.

Spectra	Intensity light (incident PPFD, μmol·m^{-2}·s^{-1})																					
	200 ppm CO_2							400 ppm CO_2							850 ppm CO_2							
	30	90	200	350	500	700	1000	30	90	200	350	500	700	1000	30	90	200	350	500	700	1000
37R36G27B	-2,36	-0,87	-0,11	0,79	1,28	0,61	1,13	-1,14	0,39	4,18	4,82	6,56	5,75	7,40	-0,08	2,59	6,46	8,23	9,34	10,39	11,32
100B	-1,17	-0,14	1,05	1,87	2,36	1,62	2,14	0,45	1,31	5,81	6,30	8,12	7,14	8,87	1,89	3,85	8,50	10,15	11,37	12,25	13,29
100G	-2,16	-0,69	0,07	0,97	1,46	0,79	1,31	-0,93	0,58	4,39	5,02	6,76	5,95	7,60	0,14	2,78	6,69	8,45	9,57	10,61	11,55
100R	-1,42	-0,11	0,32	1,44	1,53	1,18	1,35	0,01	1,24	4,99	5,67	7,23	6,49	7,96	1,34	3,62	7,85	9,50	10,70	11,57	12,59
20B80G	-1,47	-0,49	0,64	1,51	1,93	1,24	1,69	0,20	0,98	5,50	5,99	7,78	6,81	8,50	1,71	3,57	8,32	9,94	11,18	12,02	13,08
20G80R	-2,40	-0,77	-0,10	0,80	1,32	0,64	1,19	-1,30	0,43	4,04	4,72	6,44	5,68	7,32	-0,36	2,52	6,17	7,99	9,06	10,16	11,06
20R80B	-0,35	0,29	2,23	2,78	3,59	2,52	3,31	1,56	1,89	7,21	7,50	9,57	8,35	10,29	3,24	4,69	9,93	11,55	12,81	13,65	14,74
80B20G	-1,33	-0,18	0,80	1,69	2,11	1,45	1,91	0,20	1,23	5,48	6,03	7,79	6,88	8,55	1,56	3,69	8,15	9,82	11,01	11,92	12,94
80G20R	-2,25	-0,84	0,08	0,92	1,49	0,74	1,32	-0,98	0,44	4,41	5,01	6,79	5,94	7,64	0,12	2,69	6,68	8,45	9,56	10,61	11,55
80R20B	-0,80	-0,23	1,64	2,25	2,96	1,97	2,66	1,19	1,41	6,77	7,06	9,08	7,87	9,77	2,98	4,28	9,68	11,25	12,54	13,33	14,45

under the same conditions until measurements with spectrum change. Other authors studied plants grown in different conditions from the beginning of their growth. Authors such as Huber et al. (2021) studied the relationship between light intensities (three daily light integral, DLIs) and three different CO_2 concentrations but with a fixed spectrum ratio of 40B:60R. Other authors focus on the relationship between light intensities and light quality in spectra of red and blue combinations (Hernández and Kubota, 2012; Zheng et al., 2021).

In our tests, we have observed (Tables 3, 4) that the influence of intensity on parameter *d* (asymptotic value of maximum A_n when the CO_2 concentration tends to infinity) is higher than the effect of the tested spectra. The net assimilation rate (A_n) obtained in the trial was around between 11-15 μmol CO_2·m^{-2}·s^{-1} for 1000 μmol·m^{-2}·s^{-1} of PPFD. These values agree with those obtained by Yang et al. (2018) for tomato seedlings at 6-leaf stage. In our model, the *d* parameter values, when the intensities of 30 and 700 μmol·m^{-2}·s^{-1}, is 11.75 while the fluctuation of *d* as a spectrum function is 3.86. The effects of light intensity or PPFD is the primary variable to identify in the light needs of plants (DLI). Usually, increases in light intensity correlate with increases in net photosynthesis rate (A_n) (Bowes et al., 1972; Fan et al., 2013). PPFD of 700 μmol·m^{-2}·s^{-1} was the highest A_n obtained by Ke et al. (2022) compared to the intensity of 300 and 500 μmol·m^{-2}·s^{-1}. In our results, values of 700 and 1000 μmol·m^{-2}·s^{-1} were the highest A_n obtained, too.

However, at similar intensity levels, the effect of the spectrum greatly influences A_n (Table 5 and Figure 3). The best results were shown by the combination of red and blue LEDs (20B80R and 80R20R). Similar results were reported on tomato seedlings by (Hernández et al., 2016) after studying various spectra, concluding that the combinations of 30B70R and 50B50R showed a greater fresh and dry mass. However, there were no differences in A_n between the different spectra. Liu et al. (2011) indicated that the spectrum with the best performance in improving photosynthesis for tomato seedlings was the combination of RB in a 1:1 ratio with PPFD of 320 μmolm^2s^{-1}. Kaiser et al. (2019) indicated that in greenhouse tomato production, the optimal proportions of blue light are between 6-12%, while the higher values are the optimal plant growth. Liu et al. (2011) showed that of the monochromatic lights tested (blue, green, yellow and red), the one that showed the best behaviour was a blue light, coinciding with the results shown in this study (Table 7). Our results indicate that Blue light is more efficient in driving photosynthesis when comparing the three monochromatic light sources (100B>100R>100G). At the same time, photosynthesis is more efficient when Blue light is in combination with other colours, being the predominant wavelength of the mix. The absorbance values for Blue and Red light are between 80 and 95% (Terashima et al., 2009). Moreover, the limitation in one of these spectra causes photosynthesis inefficiency or other plant disorders (Hogewoning et al., 2010). This study has shown that monochromatic Red light impairs the photosynthetic machinery, reducing photosynthetic capacity in the so-called "red light syndrome" (Kaiser et al., 2019). This effect can be reverted by adding even small proportions of Blue light (Hogewoning et al., 2010). The peaks at which the LEDs used in this work emit light are closer to the absorption peak of chlorophylls

TABLE 7 Calculated A_n increment relative to that of the spectrum 37R36G27B (designed after sun radiation) at 350 µmol·m^{-2}·s^{-1} and 400 ppm of CO_2 (yellow cell) for every spectrum and intensity tested in the three theoretical CO_2 concentration scenarios of 200 ppm, 400 ppm and 700 ppm.

	Intensity light (incident PPFD, µmol·m^{-2}·s^{-1})																				
	30	90	200	350	500	700	1000	30	90	200	350	500	700	1000	30	90	200	350	500	700	1000
Spectra	200 ppm CO_2							400 ppm CO_2							850 ppm CO_2						
37R36G27B	-149	-118	-102	-84	-73	-87	-77	-124	-92	-13	0	36	19	53	-102	-46	34	71	94	115	135
100B	-124	-103	-78	-61	-51	-66	-56	-91	-73	20	31	68	48	84	-61	-20	76	110	136	154	176
100G	-145	-114	-98	-80	-70	-84	-73	-119	-88	-9	4	40	23	58	-97	-42	39	75	98	120	139
100R	-129	-102	-93	-70	-68	-76	-72	-100	-74	3	18	50	35	65	-72	-25	63	97	122	140	161
20B80G	-131	-110	-87	-69	-60	-74	-65	-96	-80	14	24	61	41	76	-65	-26	72	106	132	149	171
20G80R	-150	-116	-102	-83	-73	-87	-75	-127	-91	-16	-2	33	18	52	-107	-48	28	66	88	111	129
20R80B	-107	-94	-54	-42	-26	-48	-31	-68	-61	50	56	98	73	113	-33	-3	106	139	165	183	206
80B20G	-128	-104	-83	-65	-56	-70	-61	-96	-75	14	25	62	43	77	-68	-24	69	104	128	147	168
80G20R	-147	-117	-98	-81	-69	-85	-73	-120	-91	-9	4	41	23	58	-98	-44	38	75	98	120	139
80R20B	-117	-105	-66	-53	-39	-59	-45	-75	-71	40	46	88	63	102	-38	-11	101	133	160	176	200

A_n <-99 | -99< A_n <-66 | -66< A_n <-33 | -33< A_n <33 | 33< A_n <66 | 66> A_n <99 | 99< A_n

The font number shows whether the calculated A_n is higher (in green) or lower (in red) than the reference. The background darkness indicates whether the An value is higher (in green) or lower (in red) than that of 37R36G27B at 350 µmol·m^{-2}·s^{-1} at the same CO_2 concentration.

10.3389/fpls.2023.1327385

TABLE 8 Photosynthetic Light-Use Efficiency (PLUE, mmol CO_2/mol photon) for each light intensity and spectrum tested at three CO_2 concentration scenarios: 400 ppm as atmospheric CO2 concentration, 850 ppm as the concentration of a carbon fertilized greenhouse and 200 ppm as the case of a CO_2 deprived ambient due to a high photosynthetic rate.

Spectra	Intensity light (incident PPFD, μmol·m^{-2}·s^{-1})																			
	200 ppm CO_2							400 ppm CO_2							850 ppm CO_2						
	30	90	200	350	500	700	1000	30	90	200	350	500	700	1000	30	90	200	350	500	700	1000
37R36G27B	-78,52	-9,64	-0,55	2,26	2,57	0,87	1,13	-38,07	4,33	20,91	13,78	13,11	8,22	7,40	-2,82	28,75	32,31	23,53	18,68	14,84	11,32
100B	-38,94	-1,58	5,23	5,34	4,72	2,32	2,14	14,84	14,55	29,03	17,99	16,24	10,21	8,87	63,01	42,80	42,49	29,01	22,73	17,50	13,29
100G	-72,03	-7,66	0,37	2,79	2,93	1,13	1,31	-31,08	6,39	21,94	14,35	13,52	8,50	7,60	4,65	30,94	33,43	24,16	19,13	15,15	11,55
100R	-47,29	-1,23	1,58	4,12	3,06	1,69	1,35	0,34	13,79	24,96	16,21	14,45	9,27	7,96	44,54	40,17	39,26	27,15	21,39	16,52	12,59
20B80G	-49,07	-5,48	3,21	4,31	3,85	1,78	1,69	6,59	10,93	27,48	17,11	15,57	9,73	8,50	57,08	39,70	41,59	28,41	22,36	17,18	13,08
20G80R	-80,09	-8,59	-0,51	2,28	2,65	0,92	1,19	-43,48	4,75	20,20	13,47	12,87	8,11	7,32	-11,99	28,05	30,87	22,82	18,12	14,51	11,06
20R80B	-11,64	3,17	11,14	7,94	7,19	3,60	3,31	51,94	20,96	36,07	21,44	19,13	11,92	10,29	107,97	52,09	49,65	33,00	25,61	19,50	14,74
80B20G	-44,26	-1,96	4,02	4,84	4,22	2,07	1,91	6,52	13,65	27,42	17,23	15,58	9,83	8,55	52,14	40,99	40,74	28,05	22,03	17,03	12,94
80G20R	-75,11	-9,37	0,42	2,63	2,98	1,06	1,32	-32,80	4,93	22,05	14,32	13,59	8,49	7,64	3,85	29,89	33,40	24,14	19,12	15,15	11,55
80R20B	-26,60	-2,58	8,20	6,43	5,91	2,81	2,66	25,12	15,65	33,84	20,16	18,16	11,24	9,77	99,36	47,55	48,38	32,14	25,09	19,04	14,45
Mean	-52,36	-4,49	3,31	4,29	4,01	1,82	1,80	-4,01	10,99	26,39	16,61	15,22	9,55	8,39	41,78	38,09	39,21	27,24	21,43	16,64	12,66

10.3389/fpls.2023.1327385

in blue than in red, thus more effectively used by these pigments. This fact could explain the results obtained.

Greenlight has been proposed to drive photosynthesis more efficiently than Blue and Red light when light intensity reaches a saturating point (Terashima et al., 2009) due to the better distribution/penetration along the leaves. This effect is effectively used along the depths of the leaf and not only on the adaxial parts. However, this was not the case in this study. Greenlight reaches lower A_n values than Red and Blue light. Although, it is observed that at low intensities, the differences of A_n between Green and other spectra are more significant as the intensity of light increases (Table 6). This result could be because light saturating points have not been reached in this experiment, so all light received by leaves did not saturate the chloroplasts present on the adaxial part of leaves.

Further research should be performed at higher light intensities to determine whether higher intensities are needed to boost Green photosynthetic efficiency in tomatoes or whether this phenomenon is species-dependent and does not occur in tomato plants. One of the most critical variables in artificial lighting is PLUE, which represents the ratio between net photosynthesis and moles of photons applied. Concerning our test, it is observed that as the intensity increases, the PLUE

decreases. The values and trend shown align with those obtained by (Ke et al., 2022) with values between 30-40 with light intensities from 300 to 500 $\mu mol \cdot m^{-2} \cdot s^{-1}$ and CO_2 concentrations of 1000 ppm.

The model established in this study does not adjust properly to the cases of lower light intensity (30 and 90 µmol·m-2·s-1), showing a discreet but lineal increase of An. This might be because the CO2 saturating point is reached at low light intensities, thus skipping the exponential part of the CO2 response curves. This would be in synchrony with the assumption of not reaching the light saturation point, evidencing a high light necessity of tomato (or at least the variety studied).

5 Conclusion

The interaction between light intensity and CO_2 concentration on tomato seedlings has shown characteristic curves A_n/Light and A_n/CO_2 for all spectra. The intensity of light and the concentration of CO_2 are the parameters that most condition the A_n rate. The generated model and its parameters allow for the estimation and discrimination of the values achieved based on intensity, spectra, and CO2 concentration. For some fixed values of CO_2 concentration and with close tested light intensities, spectra with better behaviour than others have been observed, and the differences between spectra with lower light intensities were more pronounced. The spectra with better behaviour, with a higher rate of A_n, have been 20B80R and 80B20R. The tests carried out indicate that at low lighting intensities tested<350 $\mu mol \cdot m^{-2} \cdot s^{-1}$, the effect of the spectrum is more important because these increases represent a very high percentage with respect to the maximum potential of A_n. In the artificial light application industry, where the intensities are low and can never compete with those coming from natural light, spectrum choice is essential to optimize the photosynthesis of the species, as indicated by the data on photosynthetic light use efficiency in this study. It is necessary to conduct more research to evaluate the growth and development of the complete plant since, although the spectra cited (20B80R, 80B20R) show better behaviour in A_n, they can influence the morphology and growth of the plant in different ways from a crop perspective.

Data availability statement

The raw data supporting the conclusions of this article will be made available by the authors, without undue reservation.

Author contributions

RM: Conceptualization, Formal analysis, Funding acquisition, Investigation, Methodology, Supervision, Validation, Writing – original draft, Writing – review & editing, Resources, Visualization. RJ: Data curation, Formal analysis, Investigation, Writing – original draft. MMa: Data curation, Formal analysis, Project administration, Software, Visualization, Writing – original draft. MI: Data curation, Formal analysis, Methodology, Software, Validation, Writing – original draft. MMo: Conceptualization, Methodology, Resources, Writing – original draft. AT: Funding acquisition, Resources, Supervision, Validation, Visualization, Writing – review & editing, Writing – original draft.

Funding

The author(s) declare financial support was received for the research, authorship, and/or publication of this article. This research was funded by the Comunidad de Madrid project grant number IND2019/BIO-17149, Optimisation of Mediterranean horticultural production by artificial light.

Conflict of interest

The authors declare that the research was conducted in the absence of any commercial or financial relationships that could be construed as a potential conflict of interest.

Publisher's note

References

Bantis, F., Smirnakou, S., Ouzounis, T., Koukounaras, A., Ntagkas, N., and Radoglou, K. (2018). Current status and recent achievements in the field of horticulture with the use of light-emitting diodes (LEDs). *Sci. Hortic.* 235, 437–451. doi: 10.1016/J.SCIENTA.2018.02.058

Berkovich, Y. A., Konovalova, I. O., Smolyanina, S. O., Erokhin, A. N., Avercheva, O., Bassarskaya, E. M., et al. (2017). LED crop illumination inside space greenhouses. *Reach* 6, 11–24. doi: 10.1016/j.reach.2017.06.001

Both, A. J., Frantz, J. A., and Bugbee, B. (2017). "Carbon Dioxide Enrichment in Controlles Enviroments," in *LIGHT Management in Controlled Environments*. Eds. R. Lopez and E. Runkle (OH,USA: Willoughby), 82–90.

Bowes, G., Ogren, W. L., and Hageman, R. H. (1972). Light saturation, photosynthesis rate, ruDP carboxylase activity, and specific leaf weight in soybeans grown under different light intensities [1]. *Crop Sci.* 12, 77–79. doi: 10.2135/cropsci1972.0011183X001200010025x

Dorais, M., Ehret, D. L., and Papadopoulos, A. P. (2008). Tomato (Solanum lycopersicum) health components: From the seed to the consumer. *Phytochem. Rev.* 7, 231–250. doi: 10.1007/s11101-007-9085-x

Du, H., Fuh, R. C. A., Li, J., Corkan, L. A., and Lindsey, J. S. (1998). PhotochemCAD++: A computer-aided design and research tool in photochemistry. *Photochem. Photobiol.* 68, 141–142. doi: 10.1111/j.1751-1097.1998.tb02480.x

Fan, X. X., Xu, Z. G., Liu, X. Y., Tang, C. M., Wang, L. W., and Han, X. L. (2013). Effects of light intensity on the growth and leaf development of young tomato plants grown under a combination of red and blue light. *Sci. Hortic.* 153, 50–55. doi: 10.1016/j.scienta.2013.01.017

FAOSTAT (2022) *Food and Agriculture Organization of the United Nation*. Available at: https://www.fao.org/faostat/en/#data (Accessed March 31, 2022).

Farquhar, G. D., von Caemmerer, S., and Berry, J. A. (1980). A biochemical model of photosynthetic CO 2 assimilation in leaves of C 3 species. *Planta* 149 (1), 78–90. doi: 10.1007/BF00386231

Feller, C., Bleiholder, H., Buhr, L., Hack, H., He, M., Klose, R., et al (1995). Phanologische Entwicklungsstadien von Gemusepflanzen II. Fruchtgemuse und Hulsenfruchte Codierung und Beschreibung nach der erweiterten BBCH-Skala-rnit Abbildungen Phenological growth stages of vegetable crops II. *Nachrichtenbl. Deut. Pflanzenschutzd.* 47 (9), 217–232.

Hernández, R., Eguchi, T., Deveci, M., and Kubota, C. (2016). Tomato seedling physiological responses under different percentages of blue and red photon flux ratios using LEDs and cool white fluorescent lamps. *Sci. Hortic.* 213, 270–280. doi: 10.1016/j.scienta.2016.11.005

Hernández, R., and Kubota, C. (2012). Tomato seedling growth and morphological responses to supplemental LED lighting red:Blue ratios under varied daily solar light integrals. *Acta Hortic.* 956, 187–194. doi: 10.17660/ActaHortic.2012.956.19

Hogewoning, S. W., Trouwborst, G., Maljaars, H., Poorter, H., van Ieperen, W., and Harbinson, J. (2010). Blue light dose-responses of leaf photosynthesis, morphology, and chemical composition of Cucumis sativus grown under different combinations of red and blue light. *J. Exp. Bot.* 61, 3107–3117. doi: 10.1093/jxb/erq132

Huber, B. M., Louws, F. J., and Hernández, R. (2021). Impact of different daily light integrals and carbon dioxide concentrations on the growth, morphology, and production efficiency of tomato seedlings. *Front. Plant Sci.* 12. doi: 10.3389/fpls.2021.615853

Kaiser, E., Ouzounis, T., Giday, H., Schipper, R., Heuvelink, E., and Marcelis, L. F. M. (2019). Adding blue to red supplemental light increases biomass and yield of greenhouse-grown tomatoes, but only to an optimum. *Front. Plant Sci.* 9, 2002. doi: 10.3389/fpls.2018.02002

Ke, X., Yoshida, H., Hikosaka, S., and Goto, E. (2022). Optimization of photosynthetic photon flux density and light quality for increasing radiation-use efficiency in dwarf tomato under led light at the vegetative growth stage. *Plants* 11, 121. doi: 10.3390/plants11010121

Li, Y., Liu, C., Shi, Q., Yang, F., and Wei, M. (2021). Mixed red and blue light promotes ripening and improves quality of tomato fruit by influencing melatonin content. *Environ. Exp. Bot.* 185, 104407. doi: 10.1016/j.envexpbot.2021.104407

Liang, L., Zhang, Z., Cheng, N., Liu, H., Song, S., Hu, Y., et al. (2021). The transcriptional repressor OsPRR73 links circadian clock and photoperiod pathway to control heading date in rice. *Plant Cell Environ.* 44, 842–855. doi: 10.1111/pce.13987

Lindstrom, M. J., and Bates, D. M. (1990) *Nonlinear Mixed Effects Models for Repeated Measures Data*. Available at: https://www.jstor.org/stable/2532087?seq=1&cid=pdf-.

Liu, X. Y., Chang, T. T., Guo, S. R., Xu, Z. G., and Li, J. (2011). Effect of different light quality of led on growth and photosynthetic character in cherry tomato seedling. *Acta Hortic.* 905, 325–330. doi: 10.17660/ActaHortic.2011.907.53

Liu, J., and van Iersel, M. W. (2021). Photosynthetic physiology of blue, green, and red light: light intensity effects and underlying mechanisms. *Front. Plant Sci.* 12. doi: 10.3389/fpls.2021.619987

McCree, K. J. (1971). The action spectrum, absorptance and quantum yield of photosynthesis in crop plants. *Agric. Meteorology* 9, 191–216. doi: 10.1016/0002-1571(71)90022-7

Paucek, I., Pennisi, G., Pistillo, A., Appolloni, E., Crepaldi, A., Calegari, B., et al. (2020). Supplementary LED interlighting improves yield and precocity of greenhouse tomatoes in the mediterranean. *Agronomy* 10, 1002. doi: 10.3390/agronomy10071002

Pennisi, G., Blasioli, S., Cellini, A., Maia, L., Crepaldi, A., Braschi, I., et al. (2019). Unraveling the role of red:Blue LED lights on resource use efficiency and nutritional properties of indoor grown sweet basil. *Front. Plant Sci.* 10. doi: 10.3389/fpls.2019.00305

Pinheiro, J., Bates, D., DebRoy, S., and Core Team, R. (2021) *nlme: Linear and Nonlinear mixed Effects Models_*. Available at: https://CRAN.R-project.org/package=nlme.

R Core Team (2021) *R: A Language and Environment for Statistical Computing*. Available at: https://www.R-project.org.

Russell, V. L. (2022) *emmeans: Estimated Marginal Means, aka Least-Squares Means*. Available at: https://CRAN.R-project.org/package=emmeans.

Saathoff, A. J., and Welles, J. (2021). Gas exchange measurements in the unsteady state. *Plant Cell Environ.* 44, 3509–3523. doi: 10.1111/pce.14178

Sipos, L., Boros, I. F., Csambalik, L., Székely, G., Jung, A., and Balázs, L. (2020). Horticultural lighting system optimalization: A review. *Sci. Hortic.* 273, 109631. doi: 10.1016/j.scienta.2020.109631

Spalholz, H., Perkins-Veazie, P., and Hernández, R. (2020). Impact of sun-simulated white light and varied blue:red spectrums on the growth, morphology, development, and phytochemical content of green- and red-leaf lettuce at different growth stages. *Sci. Hortic.* 264, 109195. doi: 10.1016/J.SCIENTA.2020.109195

Sun, J., Nishio, J. N., and Vogelmann, T. C. (1998) *Green Light Drives CO 2 Fixation Deep within Leaves*. Available at: https://academic.oup.com/pcp/article/39/10/1020/1844911.

Terashima, I., Fujita, T., Inoue, T., Chow, W. S., and Oguchi, R. (2009). Green light drives leaf photosynthesis more efficiently than red light in strong white light: Revisiting the enigmatic question of why leaves are green. *Plant Cell Physiol.* 50, 684–697. doi: 10.1093/pcp/pcp034

Trojak, M., Skowron, E., Sobala, T., Kocurek, M., and Pałyga, J. (2022). Photosynthesis Research (2022) Effects of partial replacement of red by green light in the growth spectrum on photomorphogenesis and photosynthesis in tomato plants. *Photosynth Res.* 151, 295–312. doi: 10.1007/s11120-021-00879-3

van Iersel, M. W. (2017). "Optimizing LED lighting in controlled environment agriculture," in *Light emitting diodes for agriculture: smart lighting* (Singapore: Springer), 59–80. doi: 10.1007/978-981-10-5807-3_4

Viršilė, A., Olle, M., and Pavelas, D. (2017). "LED lighting in horticulture," in *light emitting diodes for agriculture: Smart lightin*. Ed. S. Dutta Gupta (Singapore: Springer), 334. doi: 10.1007/978-981-10-5807-3

Wickham, H. (2009). *ggplot2* (New York, NY: Springer New York). doi: 10.1007/978-0-387-98141-3

Yang, X., Xu, H., Shao, L., Li, T., Wang, Y., and Wang, R. (2018). Response of photosynthetic capacity of tomato leaves to different LED light wavelength. *Environ. Exp. Bot.* 150, 161–171. doi: 10.1016/j.envexpbot.2018.03.013

Zhen, S., Haidekker, M., and van Iersel, M. W. (2019). Far-red light enhances photochemical efficiency in a wavelength-dependent manner. *Physiol.Plant.* 167, 21–33. doi: 10.1111/ppl.12834

Zhen, S., and van Iersel, M. W. (2017). Photochemical Acclimation of Three Contrasting Species to Different light levels: implications for optimizing supplemental lighting. *J. AMER. Soc Hortic. Sci.* 142, 346–354. doi: 10.21273/JASHS04188-17

Zhen, S., van Iersel, M., and Bugbee, B. (2021). Why Far-Red Photons Should Be Included in the Definition of Photosynthetic Photons and the Measurement of Horticultural Fixture Efficacy. *Front. Plant Sci.* 12, 693445. doi: 10.3389/fpls.2021.693445

Zheng, J., Gan, P., He, D., and Yang, P. (2021). Growth and energy use efficiency of grafted tomato transplants as affected by LED light quality and photon flux density. *Agriculture* 816. doi: 10.3390/agriculture11090816